Thermal Coarsening of Supported Palladium Combustion Catalysts†

J. G. McCarty,*,‡ G. Malukhin,‡ D. M. Poojary,‡ A. K. Datye,§ and Q. Xu§

Catalytica Energy Systems, Inc., Mountain View, California 94043, and University of New Mexico, Albuquerque, New Mexico 87131

Received: March 16, 2004; In Final Form: July 21, 2004

An essential property of combustion catalysts is long-term (>8000 h) stability at high temperatures in an environment (~1 atm of both oxygen and water vapor) that aggressively promotes sintering of the supporting oxide and coarsening of the active component. Extrapolation of accelerated coarsening rate measurements, determined from shorter exposures at higher temperatures, can be made with more confidence if the physical processes of the coarsening and sintering processes were well understood. The current work examines in detail the coarsening of a high-weight-loaded palladium catalyst supported by silica-stabilized alumina at 900 °C in such an aggressive environment. The results of this investigation showed that the Pd particle size distribution was consistently log-normal for time periods from 100 to 4000 h, the mean particle growth rate was roughly inverse second-order in mean particle diameter, and the support not only sintered but also underwent phase transformation. The results implicate both coalescence and Ostwald ripening as important coarsening processes.

Introduction

Catalytic combustion is emerging as a new low-emissions technology for power generation by gas turbines. Kawasaki Heavy Industries has placed several Catalytica Energy Systems, Inc. (CESI) Xonon Cool Combustion catalyst modules in commercial service on their 1.5-MW M1A-13X gas turbine in the U.S.A.[1] Durability in the high-temperature, humid, and oxidizing combustion environment has been the most challenging problem that has slowed the development of this technology since its low NO_x emissions potential was recognized some 30 years ago.[2] If catalytic combustion technology is destined to gain significant commercial impact, catalyst life must be extended beyond the current 8000-h guarantee. Therefore, CESI has conducted numerous investigations of thermal aging in the laboratory under metallic, oxide, and cyclic conditions and verified the aging rates in several extended field tests through 4000 and 8000 h.

Understanding the coarsening mechanism of commercially viable supported metallic palladium is important for the continuing development of sintering-resistant catalysts. Most of the supported palladium catalyst in the Xonon modules remains in the oxide phase, but in the KHI M1A-13X, a significant portion of the catalyst must operate at temperatures where the oxide transforms into the more readily coarsened metallic phase. Ideally, a physically based model of the coarsening mechanism would validate observed rates of surface area loss including the impact of temperature and environmental conditions, so that extrapolation of performance to extended time periods can be made with confidence. Also, a fundamental understanding of the physical chemistry of coarsening could determine what, if any, role the support plays in slowing particle growth. Although the support may not be expected to play a significant role in vapor-driven coarsening, interfacial contact with the supporting oxide may be expected to strongly influence particle migration.

In the current work, state-of-the-art electron microscopic imaging was used to measure particle size distributions and the coarsening rate for a model palladium combustion catalyst supported by silica-stabilized alumina under accelerated thermal aging conditions. In this investigation, the powdered catalysts were aged up to 4000 h in a pressurized furnace under conditions that simulate the pressure, temperature, and gas composition seen during commercial service. The palladium metal and the supporting oxide were characterized by measurements of specific surface area, X-ray diffraction, and microreactor activity, as well as electron microscopic imaging.

Experimental Section

The 15 wt % Pd catalyst powder was prepared over a 5 wt % silica-stabilized γ-alumina support (Davison) by two-step impregnation with an aqueous palladium nitrate solution followed by oven drying at 120 °C and calcination in air to 900 °C for 10 h. The powder was aged at 900 °C over a progressive series of time periods to 4000 h in a purged, 9.5-atm internally heated furnace with 14 vol % O_2, 10 vol % H_2O, 4 vol % CO_2, 0.5 ppmv SO_2, and the balance N_2. Trace sulfur was introduced by dissolving dimethyl sulfonic oxide in the stream used to inject water vapor into a 500-mL/min flow of premixed flushing gas containing oxygen, carbon dioxide, and nitrogen. The alumina-lined aging furnace was flushed with pure N_2 before and during cooling to avoid reoxidation of the supported Pd metal particles. Powders of several catalysts were placed in alumina trays, which were stacked in the furnace in a silica−alumina tray holder.

The fresh and aged catalyst powders were characterized by hydrogen titration using the pulsed chemisorption method at 100 °C following a 30-min reduction in 1-atm H_2 at 400 °C and oxygen chemisorption at 100 °C. Total catalyst surface areas were determined by standard nitrogen BET (5-point) analysis (Micromeritics ASAP2010). The fractional volume of the silica−alumina support and estimated domain size and strain were determined by Rietveld analysis of powder X-ray diffrac-

† Part of the special issue "Michel Boudart Festschrift".
‡ Catalytica Energy Systems, Inc.
§ University of New Mexico.

10.1021/jp048822w CCC: $30.25
Published on Web 09/30/2004

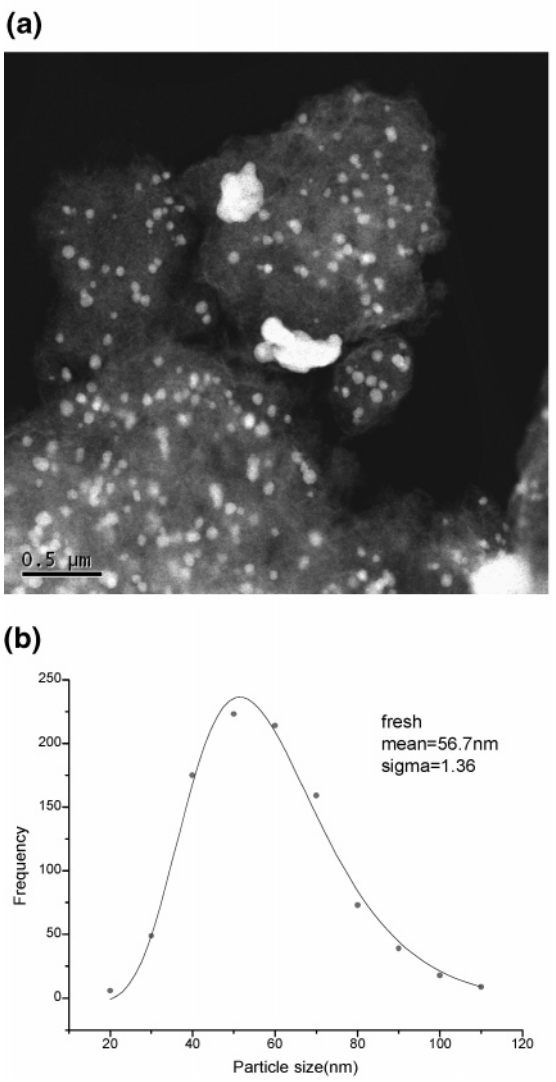

Figure 1. HADF TEM image of the fresh (nonaged) catalyst (a) and the particle size distribution derived from a set of HADF images (b).

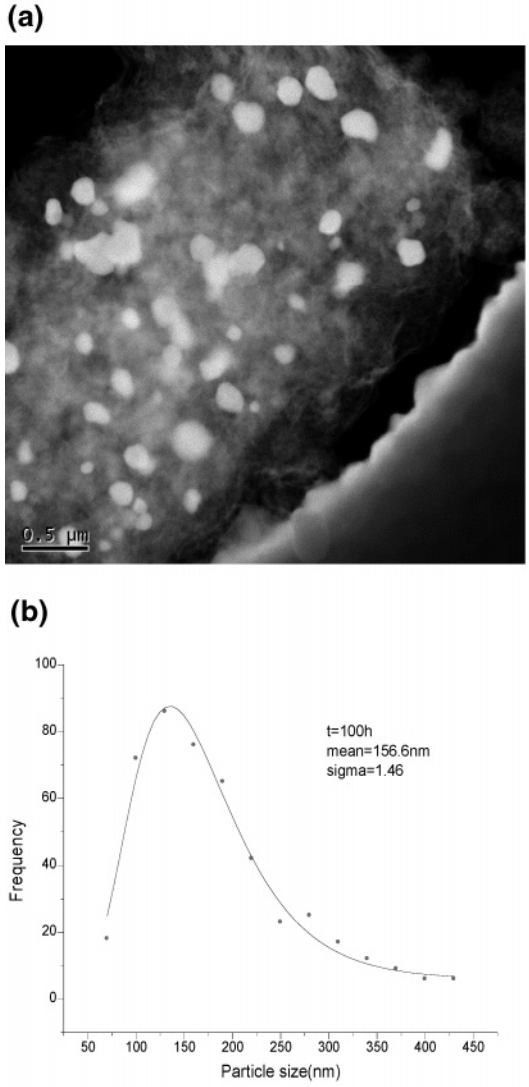

Figure 2. HADF TEM image of the 100-h aged catalyst (a) and particle size distribution derived from a set of HADF images (b).

tion (XRD) data. Step-scanned X-ray powder data were collected on the finely ground sample by means of a Scintag XDS 2000 diffractometer using Cu Kα radiation and a single-pass monochromator with solid-state detector. Data were collected between 10° and 120° in 2θ with a step size of 0.02° and a counting time of 12 s per step. The structure was refined using the program *GSAS*.[3] The refinement was started using the readily available crystallographic data (space group, unit cell parameters, positional parameters) for the α-alumina, θ-alumina, mullite, and palladium metal phases. The final cycle of Rietveld refinement converged to agreement factors of Rwp = 10.3%, Rp = 7.7%, and RF^2 = 6% (for 856 reflections).

Kinetic experiments of the aged powder samples were characterized by microreactor methane oxidation rate measurements using quartz packed-bed reactors. The reactors were fed by 600-mL/min (STP) flow consisting of 0.5 vol % of methane, 30 vol % of oxygen in helium, and 2 vol % water at a pressure of 6 atm. An on-line mass spectrometer was used to analyze reactor effluent compositions, and CH_4 conversion combustion was determined from the partial pressures of the product CO_2 and the unconverted methane. The rate constants were calculated by assuming that the reaction is first-order in methane oxidation.

The aged catalysts were also characterized by direct observation of the particle size distribution (PSD) using electron microscopy. Transmission electron microscopic (TEM) imaging of the fresh (Figure 1) and 100-h aged (Figure 2) catalysts was enhanced using the high-angle annular dark-field technique (HAADF),[4] which enabled observation of the population of particle size from <10 to 500 nm. Samples that were aged 300 , 1000 , 2000 (Figure 3), and 4000 h could be imaged adequately with high-resolution scanning electron microscopy (SEM). Other aged catalysts composed of zirconia or other dense refractory oxides cannot be imaged by TEM because of inadequate contrast from the Pd particles, but have been successfully imaged to <10 nm using high-resolution SEM.

Results and Discussion

The PSD values measured for all aged 15 wt % Pd/Si−Al_2O_3 catalysts were fitted to the log-normal distribution function with very good accuracy (Table 1). The breadth factor (σ) for the fitted distribution expressions remained constant over a wide range in mean particle size. The mean particle size and weight-normalized surface area derived from the PSD agree well with the chemisorption measurements. The mean size reported in the PSD plots is the geometric mean. Other averages such as the number average, surface average, and volume average are reported in Table 1. The surface average diameter was used to calculate the exposed metal surface area which agrees well with

TABLE 1: Log-Normal Distribution Functions and Fitting Parameters for 15 wt % Pd/Si−Alumina Catalysts Aged at 900 °C and 9.4 atm for up to 4000 h

aging time (h)	experimental data: electron microscopy					log-normal parameters		experimental measurements	
	particle count	number av size (nm)	surface av size (nm)	volume av size (nm)	exposed metal (μmol/g)	mean size (nm)	σ	exposed metal (μmol/g)	BET area (m^2/g)
0	979	54.1	69.6	81.1	22.5	56.7	1.36	21.9	142
100	461	171.3	257.1	297.3	6.1	156.6	1.46	6.3	104
300	757	349.6	451.3	497.1	3.5	388.9	1.50	3.9	80
1000	789	467.1	606.8	666.2	2.6	506.0	1.53	3.3	47
2000	609	621.5	777.5	846.0	2.0	717.7	1.55	2.5	33
4000	975	773.0	935.3	1002.8	1.7	815.2	1.43	1.8	21

the chemisorption uptake of H_2. Images of irregular particles and those showing a dumbbell shape (Figure 4) and the log-normal distributions implicate particle migration and coalescence as modes of coarsening in addition to the vaporization and migration of mobile species such as atomic Pd and $Pd(OH)_2$.

The time dependence of particle growth (Figure 5) could be represented by a coarsening rate expression following inverse second-order dependence on mean particle size, that is

$$\Delta p^2 \cdot \frac{d(\Delta p)}{dt} = k(T, y_i \cdot P) \qquad (1)$$

integrating the rate for dp and substituting $SA \propto 6 \cdot w/(dp \cdot \rho_{Pd})$, we have

$$SA(t,T, y_i \cdot P) = \left[\frac{1}{SA0^3} + k'(T, y_i \cdot P) \cdot t\right]^{-1/3} \qquad (2)$$

where dp is the mean particle size, SA is the value of exposed metal (mol/g catalyst), w the weight fraction of Pd in the catalyst, k and k' are effective coarsening rate constants, T and P are the gas temperature and pressure, respectively, and y_i is the molar fractional gas composition. After integration, the long-term values of exposed Pd (i.e., specific metallic surface area, SA)

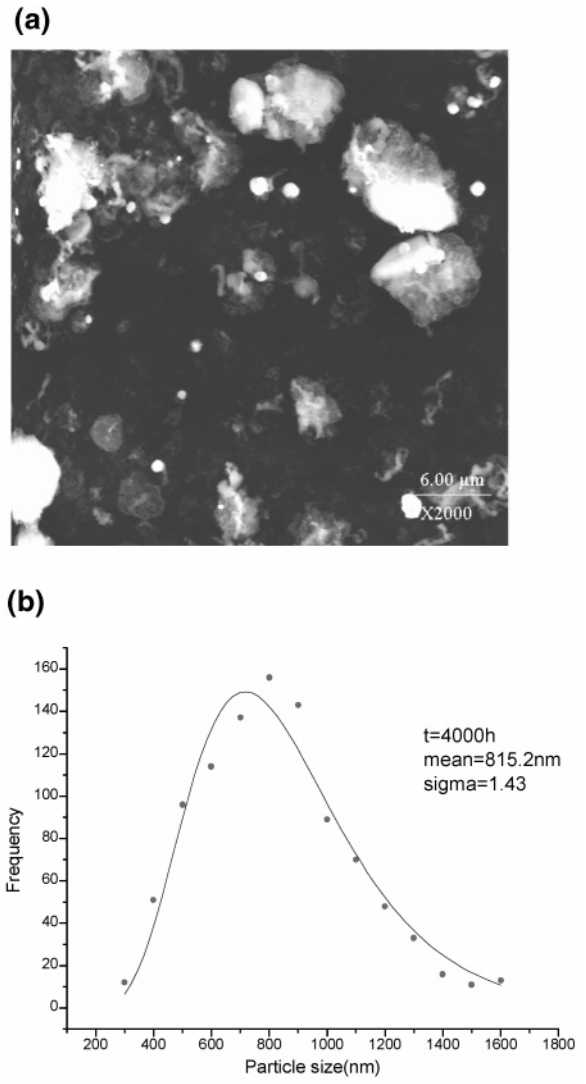

Figure 3. SEM image of the 2000-h aged catalyst (a) and particle size distribution derived from a set of SEM images (b).

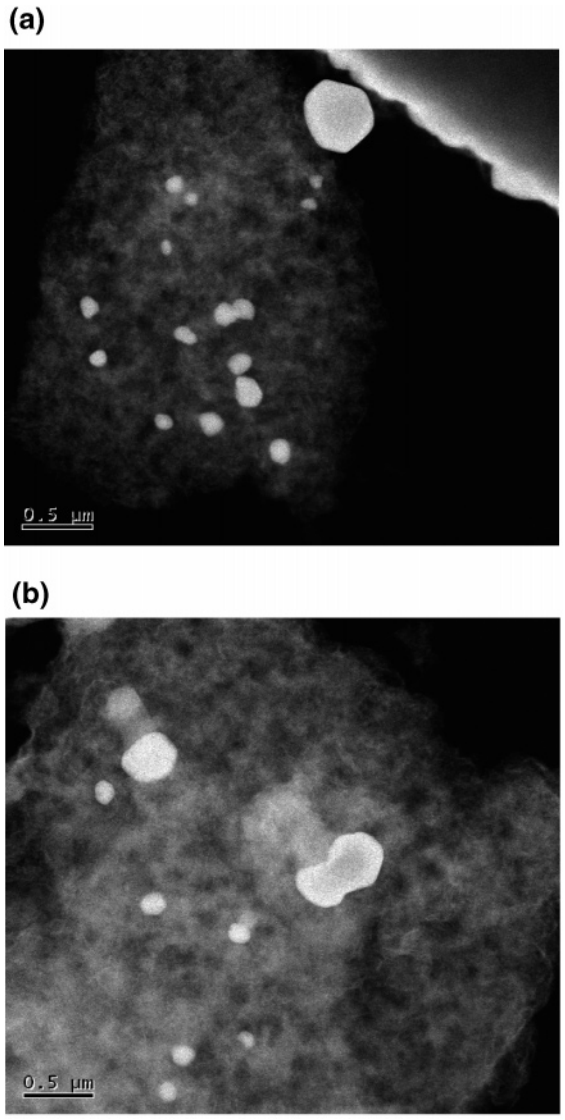

Figure 4. HADF TEM image of the 100-h aged catalyst showing faceted (a) and fused (b) particles.

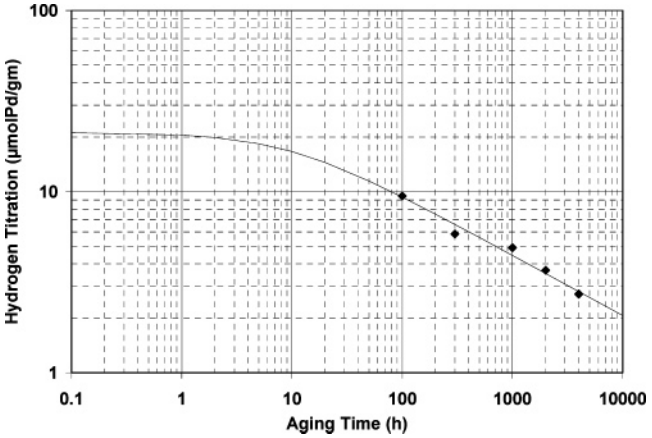

Figure 5. Logarithmic chart of the exposed Pd content (H_2 titration value) of aged catalyst powders as a function of time with the fitted integrated rate expression.

approaches SA $\propto t^{-1/3}$ without the appearance of an asymptotic limit even as the mean particle size grows to 1 μm.

Three processes appear to influence the coarsening rate: Ostwald ripening by migration of mobile species (vapor or surface diffusion); particle coalescence (fusion), perhaps more prevalent for particles <100 nm; and loss of surface area of the support by growth of α-alumina (thereby moving particles out of small pores and moving them closer to each other). It is surprising that these factors produce a very similar shape in the particle size distribution over the 15-fold increase in mean particle size and the greater than 3000-fold loss in particle count per unit volume catalyst. This may indicate that one process (vaporization) may dominate the mechanism of coarsening or that coalescence is not as size-dependent as has been postulated.[5,6]

Sintering of the support was accompanied by phase changes (from γ-alumina to a combination of mullite and θ- and α-alumina). At 4000 h, Rietveld analysis (Figure 6) showed that the support had transformed into large grains of α-alumina (phase fraction, 33 wt %), smaller mullite grains (20 wt %), and θ-alumina (33 wt %). The weight fraction for the palladium metal (14.3%) obtained from Rietveld analysis agrees well with the expected value of 15%. The electron microscopy images (see Figure 3) often show filaments pushing some Pd particles out of the support agglomerates. Perhaps the Pd metal enhances the transformation of silica-stabilized γ-alumina into threads of either θ-alumina or mullite. α-Alumina is seen as very large, nearly opaque particles. The phase transformations and significant loss of support surface area seen in the aged samples may promote particle migration by forcing particles out of mesopores and small macropores and into the macroporous voids (nominally 3 μm) between supporting oxide particles.

Microreactor tests of methane combustion activity for two of the aged samples show parallel temperature dependence (Figure 7) with the overall rate proportional to the surface area of exposed metal. This suggests that the activity is relatively structurally independent at the larger mean particle sizes examined and is only influenced by exposed Pd and not support effects (as the support transforms) or segregation of impurities. The catalysts were purged with inert gas to maintain the metallic state prior to removal from the aging furnaces and during sample heating before performing the combustion tests. The activity tests were conducted from high temperature (metallic phase) through the PdO transition at about 1.5-atm oxygen partial pressure, and a decrease in the Arrhenius slope is seen going from the metallic to the oxide regime as previously reported.[7]

The inverse second-order dependence of the rate on particle size, high apparent activation energy (~190 kJ/mol, see Figure 7), lack of variability of the rate with the nature of the support, and model studies with Pd[8−10] all strengthen the interpretation that vapor/surface monomer species migration is the primary mode of coarsening.[5−6,11] Although the particle size distributions are in line with predictions by Granqvist and Buhrmann[5] for particle migration and coalescence, the invariance of particle size distribution with growth of particle size is surprising. One would have expected that the mechanism of coarsening would switch from particle migration to Ostwald ripening as the mean particle size increased. The exponential dependence of particle size on sintering time is consistent with Ostwald ripening as the primary mechanism. Further mechanistic studies, including in situ microscopy, are in progress to further elucidate the sintering mechanism.

Summary of Findings and Conclusions

The results of the present investigation support the following conclusions.

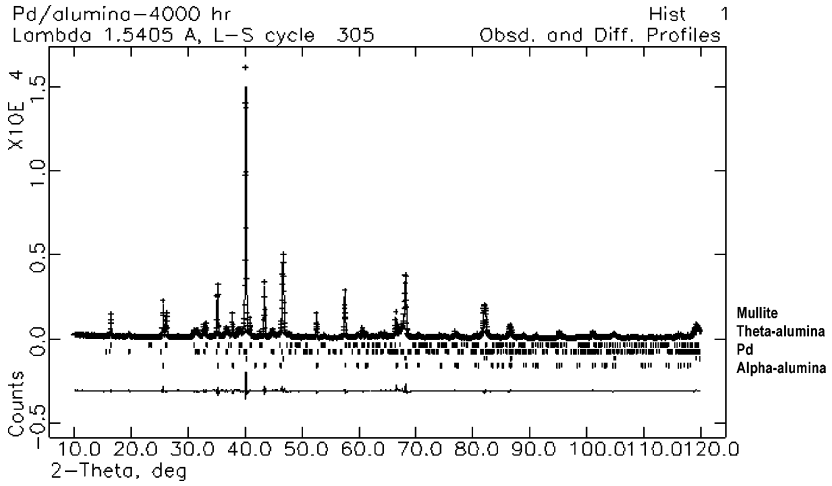

Figure 6. Observed (+) and calculated (−) profiles for the Rietveld refinement for the 4000-h aged sample. The bottom curve is the difference plot on the same intensity scale. The ticks mark the calculated positions of the possible reflections for the refined phases. The ticks from top to bottom represent the reflection positions for mullite ($Al_6Si_2O_{13}$, *Pbam*, a = 7.576(1) Å b = 7.683(1) Å 2.8859(4) Å); θ-alumina (*C*2/*m*, a = 11.791(1) Å, b = 2.9082(3) Å, c = 5.6184(5) Å, β = 103.99(1)°); palladium metal (*Fm*3*m*, a = 3.889 79(3) Å); and α-alumina (*R*3*c*, $a = b$ = 4.759 05(5) Å, c = 12.9905(2) Å).

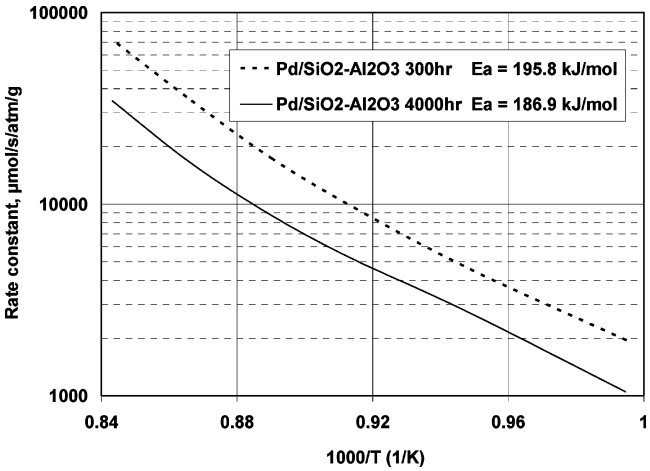

Figure 7. Effective first-order rate constant as a function of reciprocal temperature for methane oxidation over 300- and 4000-h aged catalyst samples. The rate constant for methane was determined by conversion through a packed-bed reactor.

(i) The PSD follows the log-normal distribution with a constant shape factor ($\sigma \approx 1.5$) over a 15-fold growth in mean particle size.

(ii) The coarsening rate follows approximately inverse second-order dependence on mean particle size over this growth range with no evidence of an asymptotic limit as the mean particle size approaches 1 μm.

(iii) The silica-stabilized alumina support lost 85% of its initial BET surface area and transformed into a mixture of mullite, θ-alumina, and α-alumina.

(iv) Although particle fusion was observed, the primary mechanism for Pd coarsening was vapor transport or surface diffusion of mobile species.

The task of explaining a log-normal distribution for Ostwald ripening will require further investigation.

Acknowledgment. Financial support for the work performed at UNM from the National Science Foundation, GOALI program, Grant CTS-99-11174 is gratefully acknowledged.

References and Notes

(1) See commercialization status at http://www.catalyticaenergy.com/xonon/commercialization.html.

(2) (a) Pfefferle, W. C. Catalytically Supported Thermal Combustion. U.S. Patent 3,928,961, 1975. (b) See also: Pfefferle, L. D.; Pfefferle, W. C. *Catal. Rev.—Sci. Eng.* **1987**, *29*, 219−267.

(3) Larson, A.; Von Dreele, R. B.; Lujan, M. *GSAS: Generalized Structure Analysis System*; LANSCE, Los Alamos National Laboratory, Regents of the University of California: Los Alamos, NM, 2000.

(4) Sehested, J.; Carlsson, J. A.; Janssens, T. V. W.; Hansen, P. L.; Datye, A. K. *J. Catal.* **2001**, *197*, 200−209.

(5) Granqvist, C. G.; Buhrman, R. A. *J. Catal.* **1976**, *42*, 477−479.

(6) Chakraverty, B. K. *J. Phys. Chem. Solids* **1967**, *28*, 2401.

(7) Lyubovsky, M.; Pfefferle, L.; Datye, A.; Bravo, J.; Nelson, T. *J. Catal.* **1999**, *187*, 275−284.

(8) Goeke, R. Model Supports for Studies of Catalyst Sintering. M.S. Thesis, Department of Chemical & Nuclear Engineering, University of New Mexico, Albuquerque, NM, 2003.

(9) Sanders, L. M. Diffusion of Three-Dimensional Metal Particles on an Oxide Substrate: Implications for the Sintering of Heterogeneous Catalysts. Ph.D. Thesis, Department of Chemical & Nuclear Engineering, University of New Mexico, Albuquerque, NM, 2003.

(10) Xu, Q. The Sintering of Supported Pd Automotive Catalysts. Ph.D. Thesis, Department of Chemistry, University of New Mexico, Albuquerque, NM, 2002.

(11) Wynblatt, P.; Gjostein, N. A. Supported Metal Crystallites. *Prog. Solid State Chem.* **1975**, *9*, 21−58.